MNRAS **000**, 1–7 (2016) Preprint 24 November 2016 Compiled using MNRAS LATEX style file v3.0

EPIC 220504338b: A dense hot-Jupiter transiting a solar analogue

Néstor Espinoza[1,2], Markus Rabus[1], Rafael Brahm[1,2], Matías Jones[3], Andrés Jordán[1,2], Felipe Rojas[1], Holger Drass[1], Maja Vučković[4], Joel D. Hartman[5], James S. Jenkins[6], Cristián Cortés[7,2]

[1] *Instituto de Astrofísica, Facultad de Física, Pontificia Universidad Católica de Chile, Av. Vicuña Mackenna 4860, 782-0436 Macul, Santiago, Chile.*
[2] *Millennium Institute of Astrophysics, Av. Vicuña Mackenna 4860, 782-0436 Macul, Santiago, Chile.*
[3] *European Southern Observatory, Alonso de Cordova 3107, Vitacura, Casilla 19001, Santiago 19, Chile.*
[4] *Instituto de Física y Astronomía, Facultad de Ciencias, Universidad de Valparaíso, Gran Bretaña 1111, Playa Ancha, Valparaíso 2360102, Chile.*
[5] *Department of Astrophysical Sciences, Princeton University, NJ 08544, USA.*
[6] *Departamento de Astronomía, Universidad de Chile, Camino al Observatorio 1515, Cerro Calán, Santiago, Chile.*
[7] *Departamento de Física, Facultad de Ciencias Básicas, Universidad Metropolitana de la Educación, Av. José Pedro Alessandri 774, 7760197, Ñuñoa, Santiago, Chile.*

arXiv:1611.07614v1 [astro-ph.EP] 23 Nov 2016

Accepted XXX. Received YYY; in original form ZZZ

ABSTRACT

We present the discovery of EPIC 220504338b, a dense hot-Jupiter discovered using photometry from Campaign 8 of the Kepler-2 (K2) mission and high-resolution spectroscopic follow up obtained with the FEROS spectrograph. The planet orbits a $V = 13.68$ solar analogue in a $P = 5.81771^{+0.00004}_{-0.00004}$ day orbit, has a radius of $0.91^{+0.10}_{-0.07} R_J$ and a mass of $1.28^{+0.11}_{-0.12} M_J$. With a density of $2.08^{+0.66}_{-0.57}$ gr/cm^3, the planet is among the densest systems known having masses below 2 M_J and $T_{\rm eq} > 1000$, and is just above the temperature limit at which inflation mechanisms are believed to start being important. Based on its mass and radius, we estimate that EPIC 220504338b should have a heavy element content on the order of $\sim 110\ M_\oplus$ or greater.

Key words: keyword1 – keyword2 – keyword3

1 INTRODUCTION

Transiting extrasolar planets are one of the most precious systems to discover because they allow for a wide range of characterization possibilities. Combined with radial velocity or transit timing variation analysis, the mass of these systems can be extracted, which in turn allow us to compute their densities, an important measurement that sheds light on the composition of these distant worlds.

Despite their importance, only a small fraction ($\sim 10\%$) of the currenlty ~ 2500 known transiting extrasolar planets[1] are well suited for further characterization studies, mainly because the bulk of these discoveries have been made with the original *Kepler* mission (Borucki et al. 2010), whose stars are generally too faint and most of the planets too small to characterize. Therefore, the search for transiting exoplanets around relatively bright stars is an important endeavor in which the repurposed *Kepler* mission, dubbed K2, has undoublty played an important role on, with hundreds of new systems discovered to date (see, e.g., Crossfield et al. 2016, and references therein) and many more to come.

Among the different types of transiting extrasolar planets known to date, short-period ($P \lesssim 10$), Jupiter-sized exoplanets – the so-called "hot-Jupiters" – have been one of the most studied, mainly because they are the easiest to detect and characterize. However, these are also one of the most intriguing systems to date. One of the most interesting properties of these planets is their "inflation", i.e., the fact that most of them are larger than what is expected from structure and evolution models of highly irradiated planets (Baraffe et al. 2003; Fortney et al. 2007). Although the inflation mechanism is as of today not well understood, at irradiation levels of about 2×10^8 ergs/cm^2/s (~ 1000 K) evidence suggests it stops being important (Kovács et al. 2010; Miller & Fortney 2011; Demory & Seager 2011). Planets cooler than this threshold, known as "warm" Jupiters, appear on the other hand more compact than pure H/He spheres, which in turn implies an enrichment in heavy ele-

[1] http://www.exoplanets.org, retrieved on 2016/11/19.

© 2016 The Authors

ments that most likely makes them deviate from the composition of their host stars (Thorngren et al. 2016).

Here we present a new planetary system which is in the "hot" Jupiter regime, but whose structure resembles more that of a "warm" Jupiter: EPIC 220504338b, a planet $\sim 10\%$ smaller than Jupiter but $\sim 30\%$ more massive orbiting a star very similar to our Sun. The paper is structured as follows. In Section 2 we present the data, which includes photometry from Campaign 8 of the K2 mission and spectroscopic follow-up using the FEROS spectrograph. In Section 3 we present the analysis of the data. Section 4 present a discussion and Section 5 our conclusions.

2 DATA

2.1 K2 Photometry

The candidate selection for the photometry of Campaign 8 of the K2 mission was done as described in Espinoza et al. (2016). Briefly, the photometry is first normalized with respect to any long-term variation (either of instrumental and/or stellar nature) and candidates are selected using a Box Least Squares algorithm (BLS; Kovács et al. 2002). Here we decided to obtain the photometry for the candidate selection using our own implementation of the EVEREST algorithm described in Luger et al. (2016), due to its potential of conserving stellar variability (which we filter for our candidate selection with a 20-hour median filter smoothed with a 3-hour gaussian filter, but which we also use in our analysis: see Section 3), although the full, final analysis performed here is done on the EVEREST lightcurve released at the MAST website[2]. Our candidate selection procedure identified a planetary companion candidate to the star EPIC 220504338, with a period of $\sim$5.8 days and a depth of ~ 7500 ppm. The overall precision of the lightcurve is ~ 240 ppm; the photometry is shown in Figure 1.

2.2 Spectroscopic follow-up

In order to confirm the planetary nature of our candidate, high-resolution spectroscopic follow-up was performed with the FEROS spectrograph (Kaufer & Pasquini 1998) mounted on the MPG 2.2m telescope located at La Silla Observatory in August (3 spectra) and November (6 spectra) of 2016, in order to obtain both initial stellar parameters for the candidate stellar host and high-precision radial velocity (RV) measurements. The spectra were obtained with the simultaneous calibration method, in which a ThAr calibration lamp is observed in a comparison fiber next to the science fiber, allowing us to trace instrumental RV drifts. The data was reduced with a dedicated pipeline (CERES; Jordán et al. 2014; Brahm et al. 2016a) which, in addition to the radial-velocities and bisector spans, also calculates rough atmospheric parameters for the target star. This indicated the candidate host star was a G dwarf, with an effective temperature of $T_{\rm eff} = 5500 \pm 100$ K, surface log-gravity of $\log g_* = 4.2 \pm 0.3$ dex and a metallicity of $[{\rm Fe/H}] = 0.2 \pm 0.1$ dex, all very much consistent with solar values.

[2] https://archive.stsci.edu/prepds/everest/

Table 1. Radial velocities obtained with the FEROS spectrograph along with the measured bisector spans.

Time (BJD UTC)	RV (km/s)	$\sigma_{\rm RV}$	BIS (km/s)	$\sigma_{\rm BIS}$
2457643.6804163	-41.315	0.012	-0.048	0.017
2457645.7862304	-41.236	0.010	-0.001	0.015
2457647.8755248	-41.133	0.011	0.035	0.015
2457700.7309840	-41.201	0.011	0.008	0.016
2457701.6407003	-41.313	0.010	0.031	0.015
2457702.7358066	-41.406	0.011	0.005	0.015
2457703.6386414	-41.296	0.009	-0.008	0.014
2457704.6259996	-41.137	0.013	0.038	0.013
2457705.6178241	-41.072	0.010	-0.028	0.013

The obtained RVs phased up nicely with the photometric ephemerides, hinting at a semi-amplitude of ~ 140 m/s, consistent with an object of planetary nature (see Section 3). In addition, the measured bisector spans (BIS) showed no correlation with the RVs, which is illustrated on Figure 2; performing a monte-carlo simulation by assuming the errors on the RVs and BIS are gaussian gives a correlation coefficient of $\rho = 0.15 \pm 0.16$, which is consistent with zero. The obtained radial velocities and bisector spans are presented in Table 1. These results prompted us to perform a full analysis of the system, which we present in the next section.

3 ANALYSIS

3.1 Stellar properties

In order to obtain the parameters of the host star, we first use the Zonal Atmospheric Stellar Parameters Estimator (ZASPE; Brahm et al. 2015, 2016b) algorithm. In brief, ZASPE compares the observed spectrum against a grid of stellar spectra in the most sensitive spectral zones to atmospheric parameters and determines the errors in the parameters by considering the systematic mismatch between the data and the models. In this case we run ZASPE on a high signal-to-noise (SNR; ~ 100) spectrum that was generated by co-adding the 9 individual FEROS spectra, which obtains a $T_{\rm eff} = 5627 \pm 88$ K, $\log g_* = 4.400 \pm 0.146$ dex, $[{\rm Fe/H}] = 0.180 \pm 0.062$ dex and projected rotational velocity $v\sin(i) = 2.06 \pm 0.77$ km/s, which make the host star a (slightly metal-rich) solar analogue.

In order to derive the radius, mass, age, luminosity and distance to the star, we used the latest version of the `isochrones` package (Morton 2015), which uses the derived atmospheric parameters along with photometric data in order to estimate them with evolutionary tracks. The photometric data for our star was obtained from different sources; these are presented in Table 2. We used the MESA Isochrones & Stellar Tracks (MIST; Dotter 2016; Choi et al. 2016) instead of the Darthmouth (Dotter et al. 2008) isochrones and stellar tracks, as the former cover wider ranges of radius, mass and age (although both gave results which were consistent within the errors). In order to explore the parameter space, the MULTINEST (Feroz et al. 2009) algorithm as implemented in PyMultinest (Buchner et al. 2014) was used because it is well suited for problems like the one at hand, which are inherenty degenerate. The derived stellar properties are presented in Table 2, all of which

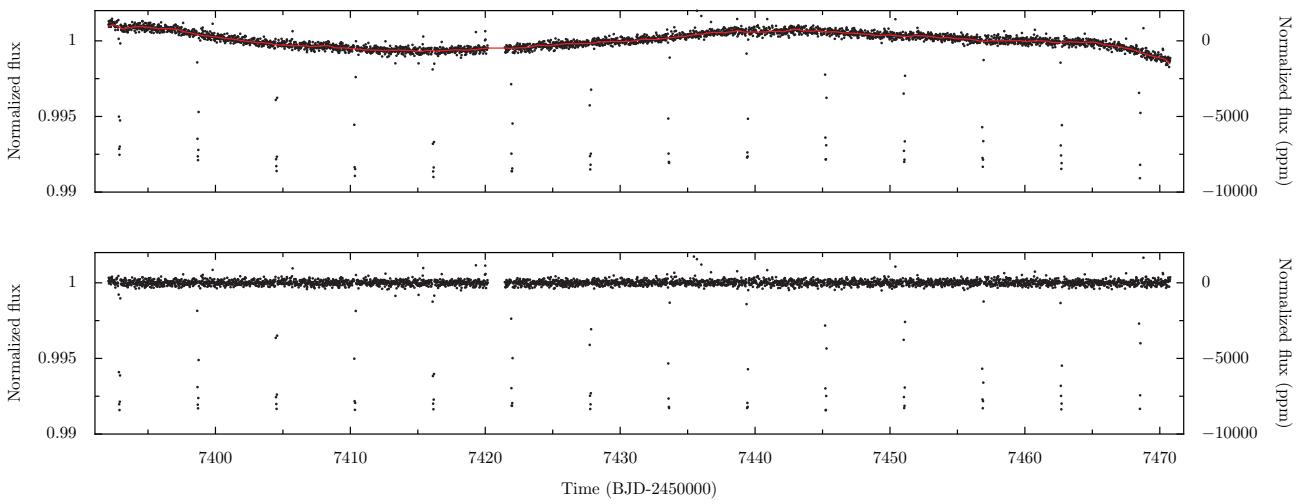

Figure 1. *Upper panel.* EVEREST photometry for the star EPIC 220504338 (black points) along with the 20-hour median filter smoothed with a 3-hour gaussian filter (red line), which captures the intrinsic variability of the star. *Lower panel.* Photometry normalized with respect to our filter.

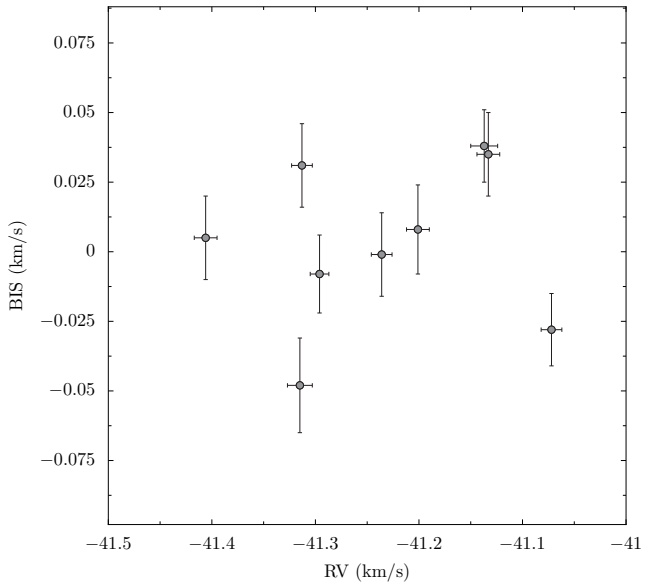

Figure 2. Radial velocity measurements versus the measured bisector spans in km/s obtained for our target star using the FEROS spectrograph. The correlation coefficient between these measurements is consistent with zero.

are consistent with the star being very similar to our own Sun ($R_* = 1.047^{+0.11}_{-0.08} R_\odot$, $M_* = 1.007^{+0.040}_{-0.039}$, $L_* = 1.02^{+0.24}_{-0.18}$). As can be observed, the only parameter that significatnly deviates (at 3-sigma) from that of a "solar twin" is the metallicity which, as mentioned above, is slighlty super-solar. We therefore consider the star a solar analogue.

3.2 Planet scenario validation

We performed a blend analysis following Hartman et al. (2011), which attempts to model the available light curves, photometry calibrated to an absolute scale, and spectroscopically determined stellar atmospheric parameters, using combinations of stars with parameters constrained to lie on

Table 2. Stellar parameters of EPIC 220504338.

Parameter	Value	Source
Identifying Information		
EPIC ID	220504338	EPIC
2MASS ID	01174783+0652080	2MASS
R.A. (J2000, h:m:s)	$01^h17^m47.829s$	EPIC
DEC (J2000, d:m:s)	$+06^o52'08.02''$	EPIC
R.A. p.m. (mas/yr)	22.3 ± 1.7	UCAC4
DEC p.m. (mas/yr)	-15.8 ± 4.1	UCAC4
Spectroscopic properties		
$T_{\rm eff}$ (K)	5627 ± 88	ZASPE
Spectral Type	G	ZASPE
[Fe/H] (dex)	0.180 ± 0.062	ZASPE
$\log g_*$ (cgs)	4.400 ± 0.146	ZASPE
$v \sin(i)$ (km/s)	2.06 ± 0.77	ZASPE
Photometric properties		
K_p (mag)	13.51	EPIC
B (mag)	14.445 ± 0.050	APASS
V (mag)	13.684 ± 0.030	APASS
g' (mag)	14.016 ± 0.030	APASS
r' (mag)	13.459 ± 0.020	APASS
i' (mag)	13.299 ± 0.030	APASS
J (mag)	12.347 ± 0.023	2MASS
H (mag)	11.998 ± 0.025	2MASS
Ks (mag)	11.949 ± 0.021	2MASS
Derived properties		
M_* ($M_\odot$)	$1.007^{+0.040}_{-0.039}$	`isochrones`*
R_* ($R_\odot$)	$1.047^{+0.11}_{-0.08}$	`isochrones`*
ρ_* (g/cm^3)	$1.23^{+0.36}_{-0.32}$	`isochrones`*
L_* ($L_\odot$)	$1.02^{+0.24}_{-0.18}$	`isochrones`*
Distance (pc)	$553.4^{+59.0}_{-43.0}$	`isochrones`*
Age (Gyr)	$5.9^{+2.7}_{-3.4}$	`isochrones`*

Note. Logarithms given in base 10.
: Using stellar parameters obtained from ZASPE.

the Girardi et al. (2000) evolutionary tracks. Possible blend scenarios include blended eclipsing binary (bEB) and hierchical triple (hEBs) systems. The analysis includes fits of the secondary eclipses and out of transit variations using the photometric data. We find that the data are best described by a planet transiting a star. All of the above mentioned blend scenarios are rejected at more than $5-\sigma$ using the photometry alone. Including the RV data, the scenarios are further ruled out: the simulated RVs for the blend model that provides the best fit to the photometric data imply variations in RV on the order of 500 m/s, which are much higher than what we observe. Based on this analysis, we consider our planet validated.

It is important to note that with our validation procedures, we can't rule out the possibility that the planetary transit is being diluted by a star whithin the 12" Kepler aperture. However, there is no known blending source within this radius in catalogs such as the Gaia Data Release 1 (Gaia Collaboration et al. 2016) and UCAC4 (Zacharias et al. 2013), while there is some stars within the 12" aperture in the Sloan Digital Sky Survey (SDSS) that have $g > 20$, which would produce negligible dilutions in the K2 lightcurve.

3.3 Joint analysis

As in Brahm et al. (2016c), the joint analysis of the K2 photometry and the FEROS RVs was performed using the EXOplanet traNsits and rAdIal veLocity fittER (EXONAILER; Espinoza et al. 2016) algorithm, which is available at GitHub[3]. The algorithm makes use of the `batman` package (Kreidberg 2015) in order to perform the transit modelling, which has the advantage of allowing the usage of any limb-darkening law, which has been proven to be of importance if unbiased transit parameters are to be retrieved from high-precision photometry (Espinoza & Jordán 2015). As recommended in the study of Espinoza & Jordán (2015), we decided to let the limb-darkening coefficients be free parameters in the fit. Following the procedures outlined in Espinoza & Jordán (2016), we concluded that the square-root law is the optimal law to use in our case, and we sampled the coefficients of this law in our joint analysis using the efficient uninformative sampling scheme outlined in Kipping (2013).

Initially, a full eccentric fit was performed but we observed the eccentricity was consistent with zero, and thus we fixed it to this value. Figure 3 shows the phase-folded photometry along with the best-fit model and Figure 4 shows the radial-velocity measurements and the corresponding best-fit model from our joint analysis. Table 3 presents the retrieved parameters. Note the moderate jitter of the star, on the order of $\sigma_{\rm RV} \sim 20$ m/s. As can be observed, the planet has a radius of $R_p = 0.91^{+0.10}_{-0.07} R_{\rm J}$, and a mass of $M_p = 1.28^{+0.11}_{-0.12} M_{\rm J}$, giving a density of $\rho_p = 2.08^{+0.66}_{-0.57}$ g/cm^3 for this planet, wich is on the high side when compared to a "typical" hot-Jupiter (where $\rho_p \lesssim 1$ g/cm^3). We discuss these planetary parameters in the context of the discovered exoplanets in the next section.

[3] https://github.com/nespinoza/exonailer

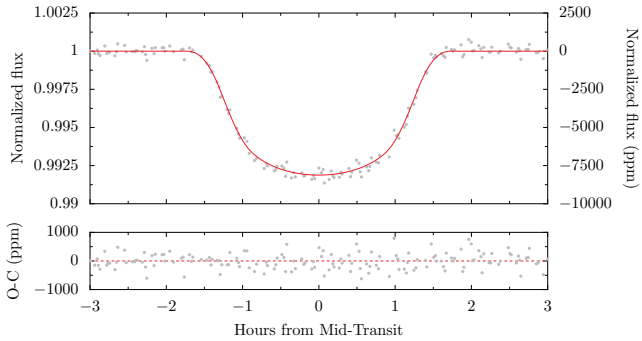

Figure 3. Phase-folded K2 photometry along with the best-fit transit model obtained from the joint analysis peformed with the EXONAILER algorithm.

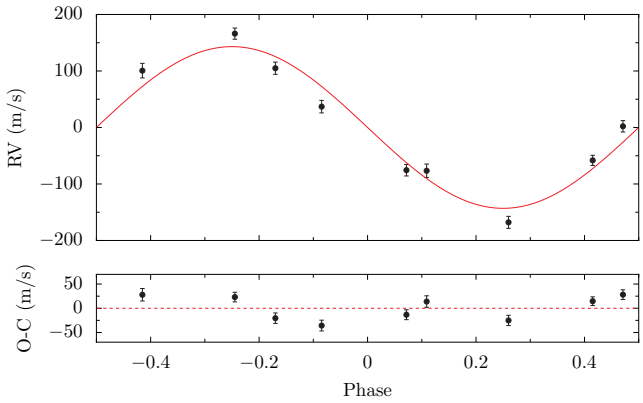

Figure 4. Phase-folded FEROS radial-velocities along with the best-fit model obtained from the joint analysis peformed with the EXONAILER algorithm.

3.4 Photometric long-term modulation in the K2 photometry

The K2 photometry presented in Figure 1 shows an evident long-term variation, which might either be interpreted as a systematic effect introduced by the EVEREST algorithm or due to intrinsic variability of the star (see Figure 5). In order to study if this could be an artifact of the detrending method, we visually inspected the Campaign 8 lightcurves using both the raw (simple aperture photometry, "SAP" flux) and EVEREST lightcurves. We observed that, for some lightcurves where there is no apparent modulation in the raw data, EVEREST can indeed introduce long-term shapes that appear like variability in the final lightcurves. In addition, the data reduced with the Presearch Data Conditioning (PDC) algorithm (Stumpe et al. 2012; Smith et al. 2012) does not show the same level of long-period variability observed in the EVEREST lightcurve, but instead shows a shorter, $\sim$ 20-day variability instead. For comparison, a periodogram analysis on the data shown in Figure 5 using the Generalized Least Squares (GLS; Zechmeister & Kürster 2009) algorithm, indicates a 55-day periodicity, which would anyways be a rare astrophysical signal for a solar analogue such as EPIC 220504338. Given all this, we conclude it is unlikely for this signal to be astrophysical in nature, and suggest caution on the interpretation of low-frequency signals in the EVEREST K2 photometry as such.

Table 3. Orbital and planetary parameters for EPIC 220504338b.

Parameter	Prior	Posterior Value
Lightcurve parameters		
P (days)	$\mathcal{N}(5.8177, 0.1)$	$5.817712^{+0.000040}_{-0.000040}$
$T_0 - 2450000$ (BJD)	$\mathcal{N}(7392.88575, 0.1)$	$7392.88588^{+0.00032}_{-0.00031}$
$a/R_\star$	$\mathcal{U}(1, 15)$	$11.74^{+0.90}_{-0.66}$
$R_p/R_\star$	$\mathcal{U}(0.01, 0.2)$	$0.0896^{+0.0015}_{-0.0024}$
i (deg)	$\mathcal{U}(70, 90)$	$86.44^{+0.54}_{-0.42}$
q_1 [a]	$\mathcal{U}(0, 1)$	$0.73^{+0.18}_{-0.18}$
q_2 [a]	$\mathcal{U}(0, 1)$	$0.23^{+0.15}_{-0.14}$
σ_w (ppm)	$\mathcal{J}(10, 500)$	$237.8^{+4.1}_{-4.0}$
RV parameters		
K (m s^{-1})	$\mathcal{N}(0, 100)$	$143.56^{+12.3}_{-12.9}$
μ (km s^{-1})	$\mathcal{N}(-41.24, 0.01)$	$-41.2379^{+0.0064}_{-0.0067}$
$\sigma_{\rm RV}$ (m s^{-1})	$\mathcal{J}(1, 100)$	$23.9^{+9.8}_{-6.6}$
e	—	0 (fixed)
Derived Parameters		
M_p ($M_{\rm J}$)	—	$1.28^{+0.11}_{-0.12}$
R_p ($R_{\rm J}$)	—	$0.91^{+0.10}_{-0.07}$
ρ_p (g/cm^3)	—	$2.08^{+0.66}_{-0.57}$
$\log g_p$ (cgs)	—	$3.58^{+0.08}_{-0.10}$
a (AU)	—	$0.0575^{+0.0074}_{-0.0057}$
$\log\langle F\rangle$ (cgs)[b]	—	$8.617^{+0.053}_{-0.066}$
$V_{\rm esc}$ (km/s)	—	$70.3^{+4.6}_{-4.6}$
$T_{\rm eq}$ (K)		
Bond albedo of 0.0	—	1163^{+38}_{-43}
Bond albedo of 0.75	—	822^{+27}_{-31}

Note. Logarithms given in base 10. $\mathcal{N}(\mu, \sigma)$ stands for a normal prior with mean μ and standard-deviation σ, $\mathcal{U}(a, b)$ stands for a uniform prior with limits a and b and $\mathcal{J}(a, b)$ stands for a Jeffrey's prior with the same limits. Times are given in BJD TBD.
[a]Triangular sampling coefficients used to fit for the square-root limb-darkening law (Kipping 2013). The s_1 and s_2 limb-darkening coefficients can be recovered by the transformation $s_1 = \sqrt{q_1}(1 - 2q_1)$ and $s_2 = 2\sqrt{q_1}q_2$.
[b]Orbit averaged incident stellar flux on the planet.

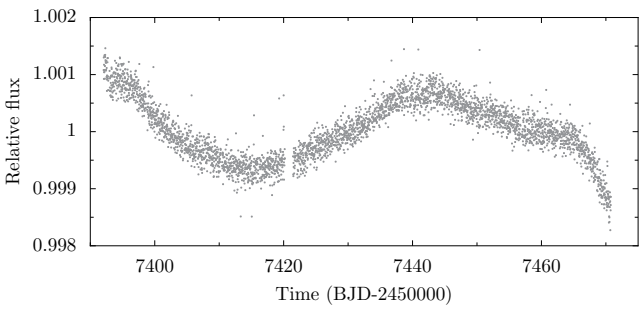

Figure 5. Long-term variation observed in the K2 photometry for our star (transits have been removed for clarity). A periodogram analysis suggests a period of $P \sim 55$ days, although it is unlikely this signal has astrophysical origin.

3.5 Searching for additional signals in the K2 photometry

The K2 photometry was inspected in order to search for additional transiting planets, secondary eclipses and/or optical phase variations. After masking out the transits, the BLS algorithm was used in order to search for additional transiting planets, but no additional signals were found. Given the lightcurve precision is 238 ppm (Table 3), our data rule out any companion larger than $\sim 3R_\oplus$ at 3-sigma with periods $P \lesssim 39$ days. As for secondary eclipses, we ran an eclipse fit at the expected times, fixing all parameters except for the planet-to-star flux ratio, F_p/F_* (allowing for negative fluxes, in order to not bias our possible detections). The retrieved flux ratio was $F_p/F_* = -32 \pm 119$ ppm, which is consistent with a non-detection. This was expected, as any secondary

eclipse would have to be smaller than $(R_p/a)^2 \sim 60$ ppm which, as can be observed, is undetectable in our case. Optical phase variations were not detected either, which was expected for similar reasons.

4 DISCUSSION

Figure 6 puts the newly discovered planet in the context of the population of known hot-Jupiters in the mass-radius diagram (left panel, $P \lesssim 10$ days, $M \gtrsim 0.1 M_J$) and of the known hot and warm Jupiters in the equilibrium temperature-radius diagram (right panel). As can be observed, EPIC 220504338b falls on a region in the mass-radius diagram that is currently not very well populated, and which hosts the densest hot-Jupiters with masses below $2M_J$ (~ 2 gr/cm^3). In the equilibrium temperature-radius diagram, on the other hand, it falls on the typical sizes of warm Jupiters, despite the fact that EPIC 220504338b would be typically classified as being "hot" due to its orbit-averaged flux of $\langle F \rangle = 4 \times 10^8$ ergs/cm^2/s, which is above (but very close to) the 2×10^8 ergs/cm^2/s threshold where it is believed "inflation" machanisms of giant planets stop being important (Miller & Fortney 2011; Demory & Seager 2011). Using the relations of Enoch et al. (2012), EPIC 220504338b would be expected to have a radius of $\sim 1.11 R_J$, which is anyways consistent (at 2-sigma) with the measured radius.

The mass and radius of EPIC 220504338b could be explained in terms of the ammount of heavy elements in the planet. In Figure 6, we see that our planet falls just where the planet evolution models of Fortney et al. (2007) predict it to be if it had a $100 M_\oplus$ core, which is a proxy for the ammount of heavy elements in the planet. Of course, giant planets are probably not just H/He envelopes sitting on top of a heavy-element core. As shown by Thorngren et al. (2016), heavy-element enrichment of the envelope is also a very important factor to take into account, although difficult to estimate based on planetary mass alone due to the high scatter in the planetary mass-heavy element relation derived in that work. For example, using this relation (which was derived from a sample of cool ($T \lesssim 1000$ K) giant planets), where a $10 M_\oplus$ heavy-element core is assumed, the ammount of heavy elements present in the envelope of EPIC 220504338b could be anywhere from $\sim 30 M_\oplus$ to $\sim 120 M_\oplus$ at 1-sigma.

Instead of trying to estimate the heavy element mass in EPIC 220504338b directly, we can compare it in terms of its radius and mass to the "warm" Jupiter WASP-130b ($M_p = 1.23 \pm 0.04 M_J$ and $R_p = 0.89 \pm 0.03 R_J$ Hellier et al. 2016). This comparison is interesting because WASP-130b is probably not affected by any inflation mechanisms due to its low irradiation levels. Because of this, Thorngren et al. (2016) was able to use structure models in order to estimate a heavy element mass of $\sim 110 M_\oplus$ for WASP-130b based on its mass and radius. Assuming that the ages of both systems are similar, we can use the heavy element mass estimated for WASP-130b as a lower limit on the heavy element mass of EPIC 220504338b. Another interesting comparison is CoRoT-13b ($M_p = 1.31 \pm 0.07$ and $R_p = 0.885 \pm 0.014$ Cabrera et al. 2010), which is the closest planet in mass and radius to EPIC 220504338b among the known hot-Jupiters, despite the fact that the former orbits a hotter star and, hence, has a larger equilibrium temperature (1700 K). This difference again could be explained in terms of the ammount of heavy elements in these planets, with EPIC 220504338b having a lower ammount than CoRoT-13b, which is estimated to have between $\sim 140 - 300 M_\oplus$ of heavy elements, which sets the upper limit on the heavy element content of EPIC 220504338b. The difference in heavy element content between WASP-130b, EPIC 220504338b and CoRoT-13b would most likely be a signature of their different formation histories rather than a correlation with other physical parameters of the system, such as the metallicities of the parent stars, whose correlation with the heavy element content on a given planet is rather weak (Thorngren et al. 2016). In fact, in this case the metallicity of WASP-130 is the largest of the three, while the metallicity of CoRoT-13 is the smallest, which casts further doubts on the prediction power of such a correlation if it were to exist.

5 CONCLUSIONS

In this work, we have presented the discovery of EPIC 220504338b, a new hot-Jupiter orbiting a slightly metal rich solar analogue discovered using photometry from Campaign 8 of the K2 mission and follow-up radial velocities using the FEROS spectrograph. The planet has a radius of $R_p = 0.91^{+0.10}_{-0.07} R_\mathrm{J}$, and a mass of $M_p = 1.28^{+0.11}_{-0.12} M_\mathrm{J}$. With a density of $2.08^{+0.66}_{-0.57}$ gr/cm^3, the planet is denser than most hot-Jupiters with masses under $2M_J$. We explain its mass and radius in terms of the amount of heavy elements in the planet, which should be on the order of $\sim 110 M_\oplus$ or greater.

ACKNOWLEDGEMENTS

N.E. is supported by the CONICYT-PCHA/Doctorado Nacional graduate fellowship. N.E., R.B., A.J. and C.C. acknowledge support from the Ministry for the Economy, Development, and Tourism Programa Iniciativa Científica Milenio through grant IC 120009, awarded to the Millennium Institute of Astrophysics (MAS). A.J. acknowledges support from FONDECYT project 1130857 and from BASAL CATA PFB-06. Support for C. C. is provided by Proyecto FONDECYT Iniciación a la Investigación 11150768.

REFERENCES

Baraffe I., Chabrier G., Barman T. S., Allard F., Hauschildt P. H., 2003, A&A, 402, 701
Borucki W. J., et al., 2010, Science, 327, 977
Brahm R., et al., 2015, AJ, 150, 33
Brahm R., Jordán A., Espinoza N., 2016a, preprint, (arXiv:1609.02279)
Brahm R., Jordan A., Hartman J., Bakos G., 2016b, preprint, (arXiv:1607.05792)
Brahm R., et al., 2016c, PASP, 128, 124402
Buchner J., et al., 2014, A&A, 564, A125
Cabrera J., et al., 2010, A&A, 522, A110
Choi J., Dotter A., Conroy C., Cantiello M., Paxton B., Johnson B. D., 2016, ApJ, 823, 102
Crossfield I. J. M., et al., 2016, ApJS, 226, 7
Demory B.-O., Seager S., 2011, ApJS, 197, 12
Dotter A., 2016, ApJS, 222, 8

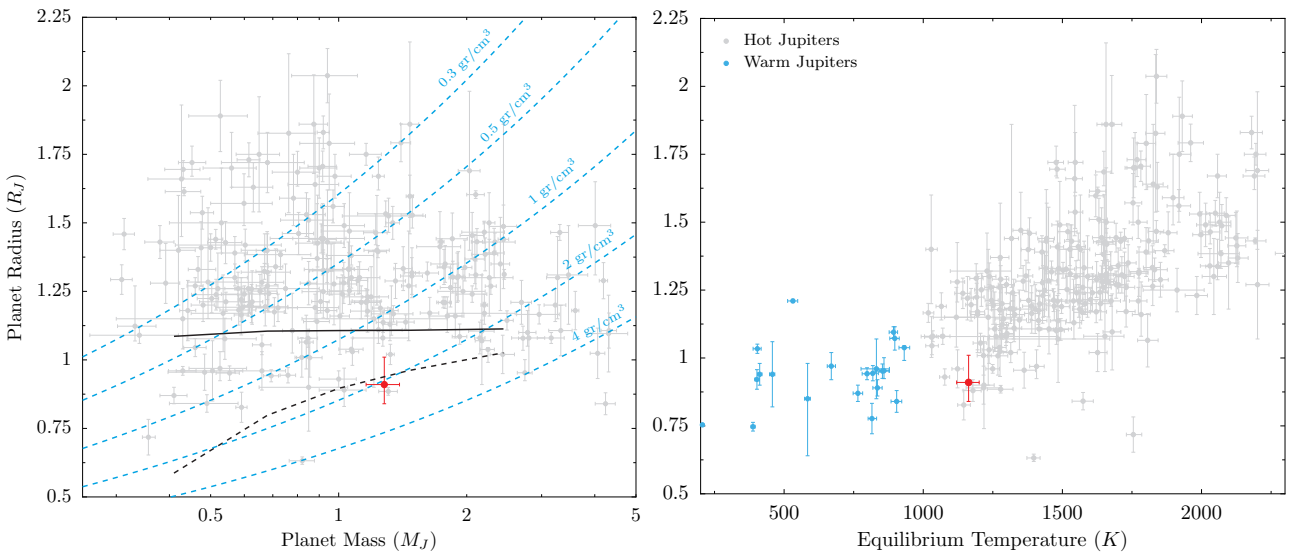

Figure 6. *Left.* Mass-radius diagram for known hot-Jupiters (grey points), along with iso-density curves (blue dashed lines) and the expected mass-radius relation for 4.5 Gyr planets at 0.045 AU from the Sun with no core (black, dashed line) and a $100M\oplus$ core (black, solid line). EPIC 220504338b is indicated as the red point with errorbars. *Right.* Equilibrium temperature-radius diagram of known hot-Jupiters (grey points) and warm Jupiters (blue points), for comparison. Again, EPIC 220504338b is depicted as a red point with errorbars.

Dotter A., Chaboyer B., Jevremović D., Kostov V., Baron E., Ferguson J. W., 2008, ApJS, 178, 89
Enoch B., Collier Cameron A., Horne K., 2012, A&A, 540, A99
Espinoza N., Jordán A., 2015, MNRAS, 450, 1879
Espinoza N., Jordán A., 2016, MNRAS, 457, 3573
Espinoza N., et al., 2016, ApJ, 830, 43
Feroz F., Hobson M. P., Bridges M., 2009, MNRAS, 398, 1601
Fortney J. J., Marley M. S., Barnes J. W., 2007, ApJ, 659, 1661
Gaia Collaboration Brown A. G. A., Vallenari A., Prusti T., de Bruijne J., Mignard F., Drimmel R., co-authors ., 2016, preprint, (arXiv:1609.04172)
Girardi L., Bressan A., Bertelli G., Chiosi C., 2000, A&AS, 141, 371
Hartman J. D., et al., 2011, ApJ, 742, 59
Hellier C., et al., 2016, preprint, (arXiv:1604.04195)
Jordán A., et al., 2014, AJ, 148, 29
Kaufer A., Pasquini L., 1998, in D'Odorico S., ed., Proc. SPIEVol. 3355, Optical Astronomical Instrumentation. pp 844–854
Kipping D. M., 2013, MNRAS, 435, 2152
Kovács G., Zucker S., Mazeh T., 2002, A&A, 391, 369
Kovács G., et al., 2010, ApJ, 724, 866
Kreidberg L., 2015, PASP, 127, 1161
Luger R., Agol E., Kruse E., Barnes R., Becker A., Foreman-Mackey D., Deming D., 2016, AJ, 152, 100
Miller N., Fortney J. J., 2011, ApJ, 736, L29
Morton T. D., 2015, isochrones: Stellar model grid package, Astrophysics Source Code Library (ascl:1503.010)
Smith J. C., et al., 2012, PASP, 124, 1000
Stumpe M. C., et al., 2012, PASP, 124, 985
Thorngren D. P., Fortney J. J., Murray-Clay R. A., Lopez E. D., 2016, ApJ, 831, 64
Zacharias N., Finch C. T., Girard T. M., Henden A., Bartlett J. L., Monet D. G., Zacharias M. I., 2013, AJ, 145, 44
Zechmeister M., Kürster M., 2009, A&A, 496, 577

This paper has been typeset from a TEX/LATEX file prepared by the author.